Electronic Supplementary Material (ESI) for Molecular Systems Design & Engineering.

Electronic Supplementary Information: Salt permeation mechanisms in charge-patterned mosaic membranes

Mark J. Summe,[1] Sushree Jagriti Sahoo,[2] Jonathan K. Whitmer,[1] and William A. Phillip[1]

[1] *University of Notre Dame, Department of Chemical and Biomolecular Engineering, Notre Dame, IN 46556.*
[2] *Indian Institute of Technology Delhi, Department of Chemical Engineering, Delhi, India.*

This document contains additional methodological details and data, as discussed in the main text.

I. MATERIALS AND METHODS

A. Diffusion Experiments

Diffusion cell experiments took place in homebuilt glass cells Fig. S1 that consisted of two well-stirred reservoirs with a membrane clamped between the reservoirs. One reservoir contained a salt solution (*i.e.*, the upstream solution) and the other reservoir contained DI water (*i.e.*, the downstream solution). The concentration of salt in the downstream reservoir was monitored over time using an Oakton Con 11 conductivity probe and this measurement was corroborated with measurements made using a Perkin Elmer Prep 3 inductively coupled plasma optical emission spectrometer (ICP-OES).

Assuming pseudo-steady-state permeation, the permeability coefficient was found by plotting the data in the form [1]:

$$\ln\left(\frac{c^0_{1,up}-c^0_{1,down}}{c_{1,up}-c_{1,down}}\right)=P\left[\frac{A_m}{\ell}\left(\frac{1}{V_{up}}+\frac{1}{V_{down}}\right)\right]t \tag{S1}$$

where the numerator and denominator of the natural log term is the difference of the concentrations in the upstream and downstream at time $t=0$ and at time t, respectively, A_m is the membrane area, ℓ is the membrane thickness, V_{up} and V_{down} are the volumes of the upstream and downstream solutions, respectively, and P is the permeability coefficient. Therefore, permeability can be calculated by plotting the natural log term as a function of t, and dividing the slope by the geometric constants in brackets.

These experiments were carried out with feed solutions that contained one of four salts: KCl, K_2SO_4, $MgCl_2$, or $MgSO_4$. In these experiment, a single salt was dissolved in the feed solution at a concentration that ranged from 1 mM to 100 mM. The permeation experiments were repeated on multiple samples of each membrane type.

B. Sorption Experiments

Multiple samples for each membrane type were soaked in solutions of either 1, 10, or 100 mM KCl, K_2SO_4, $MgCl_2$, and $MgSO_4$ for at least 4 h. Following this absorption step, membrane samples were dabbed dry with a laboratory tissue to remove residual solution and placed in a basic or acidic solution to desorb the membranes' counter-ions. Cationic membranes were placed in 10 mM NaOH to desorb the membrane counter-ions (*i.e.*, anions). The concentration of desorbed anions were measured using a Dionex ICS 5000 ion chromatograph. Anionic and uncharged membranes were placed in 10 mM HNO_3 to desorb the cations. The concentraitons of these cations were measured using ICP-OES. This procedure was carried out twice for charge-patterned mosaic membranes. First, the mosaics were placed in the NaOH solution to desorb anions. This was followed by placing the mosaics in the HNO_3 solution to desorb cations. Volumes of the desorption solution were chosen strategically to ensure concentrations were above detection limit but low enough to ensure complete desorption. Typical volumes of the desorption solution ranged from 1 mL to 20 mL for the 1 mM to 100 mM experiments. This process was carried out at least twice to ensure both reproducibility of the printing and sorption procedures.

C. Streaming Current and Conductivity Measurements

A home-built apparatus was used to measure both streaming current and ionic conductivity of the membranes. This involved placing the membrane between two reservoirs both filled with the same salt solution while a Ag/AgCl electrode was placed in each reservoir. A 10 mM KCl solution was used for the streaming current measurements. A pressure of 15 psig, measured by a pressure transducer (Omega Engineering, PX409) was applied to drive flow across the membrane while the current moving through the system was measured using the electrodes that were connected to a Keithley 2400 sourcemeter. Due to the arrangement of the electrodes in the set-up, a negative streaming current indicates a positive surface charge and a positive streaming current indicates a negative surface charge.

To determine conductivity, reservoirs were filled with varying concentrations of KCl. No pressure was applied across the membrane. Rather, voltage was varied and current measured. Conductivity (*i.e.*, the slope of the IV curve) was measured and recorded for each of these salts over a concentration range of 0.1 mM to 100 mM. This process was repeated for the three types of charged membranes (*i.e.*, positively-charged, negatively-charged, and charge-patterned mosaic membranes).

II. DETAILED THEORETICAL APPROACH

Using the assumptions enumerated in the main text, the flux of salt through the uncharged, single-charge, and charge-patterned mosaic membranes can be derived. Assuming electroneutrality within the volume of the membrane, V, implies

$$\int_V \left(\sum_i^{1,2} z_i c_i \left(\vec{r}\right) + \chi\left(\vec{r}\right) \right) d\vec{r} = 0 \tag{S2}$$

where c_i is the concentration inside the membrane, z_i is the charge on the ion. The subscripts 1 and 2 denote the cation and anion, respectively. $\chi\left(\vec{r}\right)$ represents the finite concentration of fixed charge groups within the membrane. As expressed in the main text, $\chi = 0$ for the uncharged membrane. For a membrane with a single charge, the sign of χ is determined by the local chemical composition (*e.g.* $\chi > 0$ for a positively charged membrane). In constrast, χ is a funciton of the x direction for the charge-patterned mosaic membrane.

In the absence of convection, the Nernst-Planck equation for the molar flux of an ion simplifies to

$$j_i\left(\vec{r}\right) = -D_i \left[\nabla c_i\left(\vec{r}\right) + \frac{z_i \mathcal{F} c_i\left(\vec{r}\right)}{RT} \nabla \phi\left(\vec{r}\right) \right] \tag{S3}$$

where D_i is the diffusion coefficient, ∇c_i is the concentration gradient, $\mathcal{F}$ is the Faraday constant, R is the universal gas constant, T is the temperature, and $\nabla\phi$ is the electrostatic potential gradient. Without an external potential applied across the membranes, the net ionic current through the membrane surface, S, can be assumed to be zero.

$$I = 0 = \int_S \left(\sum_i^{1,2} z_i \mathcal{F} j_i\left(\vec{r}\right) \right) d\vec{r} = 0 \tag{S4}$$

For simplicity, we will assume a symmetric salt (*i.e.* $z_1 = -z_2 = z$). For membrane samples significantly larger than the stripe width, Equations S3 and S4 are combined to solve for the diffusion potential, $\nabla\phi\left(\vec{r}\right)$

$$0 = -D_1 z \nabla c_1\left(\vec{r}\right) - z^2 D_1 c_1\left(\vec{r}\right) \frac{\mathcal{F}}{RT} \nabla\phi + D_2 z \nabla c_2\left(\vec{r}\right) + z^2 D_2 c_2\left(\vec{r}\right) \frac{\mathcal{F}}{RT} \nabla\phi \tag{S5}$$

$$\nabla\phi = -\frac{RT}{\mathcal{F}} \left(\frac{z D_1 \nabla c_1\left(\vec{r}\right) - z D_2 \nabla c_2\left(\vec{r}\right)}{z^2 D_1 c_1\left(\vec{r}\right) + z^2 D_2 c_2\left(\vec{r}\right)} \right) \tag{S6}$$

Substituting Equation S6 into Equation S3 and rearranging yields

$$j_i\left(\vec{r}\right) = j_2\left(\vec{r}\right) = -D_1 D_2 \left(\frac{c_2\left(\vec{r}\right) \nabla c_1\left(\vec{r}\right) + c_1\left(\vec{r}\right) \nabla c_2\left(\vec{r}\right)}{D_1 c_1\left(\vec{r}\right) + D_2 c_2\left(\vec{r}\right)} \right) \tag{S7}$$

Given the symmetric salt assumption, the charge balance constraint becomes

$$0 = z c_1\left(\vec{r}\right) - z c_2\left(\vec{r}\right) + \chi\left(\vec{r}\right) \tag{S8}$$

which for a membrane that is uniformly charged (or uncharged) implies that $\nabla c_2\left(\vec{r}\right) = \nabla c_1\left(\vec{r}\right)$. Using these constraints and rearranging, we have

$$j_1\left(\vec{r}\right) = -D_1 D_2 \left(\frac{2c_1\left(\vec{r}\right) + \left(\frac{\chi\left(\vec{r}\right)}{z}\right)}{\left(D_1 + D_2\right) c_1\left(\vec{r}\right) + D_2 \left(\frac{\chi\left(\vec{r}\right)}{z}\right)} \right) \nabla c_1\left(\vec{r}\right) \ , \tag{S9}$$

$$j_2\left(\vec{r}\right) = -D_1 D_2 \left(\frac{2c_2\left(\vec{r}\right) - \left(\frac{\chi\left(\vec{r}\right)}{z}\right)}{\left(D_1 + D_2\right) c_2\left(\vec{r}\right) - D_1 \left(\frac{\chi\left(\vec{r}\right)}{z}\right)} \right) \nabla c_2\left(\vec{r}\right) \ . \tag{S10}$$

For an uncharged membrane (*i.e.* $\chi\left(\vec{r}\right) = 0$), Equations S9 and S10 simplify to

$$j_1\left(\vec{r}\right) = -\left(\frac{2D_1 D_2}{D_1 + D_2} \right) \nabla c_1\left(\vec{r}\right) \tag{S11}$$

$$j_2\left(\vec{r}\right) = -\left(\frac{2D_1 D_2}{D_1 + D_2} \right) \nabla c_2\left(\vec{r}\right) \tag{S12}$$

Integrating Equation S9 over the membrane thickness for a positively-charged, single-charge membrane (*i.e.* $\chi(\vec{r}) > 0$) yields

$$j_1 = \frac{-D_1 D_2}{l}\left(\frac{(D_1 - D_2)\chi \ln\left(\frac{D_2\chi}{(D_1+D_2)c_1^m + D_2\chi}\right) - 2(D_1+D_2)c_1^m}{(D_1+D_2)^2}\right) \tag{S13}$$

In this form, it is readily seen that the expression reduces to the uncharged limit, subject to the assumption that $D_1 = D_2$. Even outside of this limit, the natural log term contributes minimally to the molar flux of the salt.

For the membranes with a charge-patterned structure, the fluxes of ions through the two oppositely-charged domains must be taken into account. Again, a subscript of $i = 1$ defines a cation, while the subscript $i = 2$ denotes an anion. The superscripts $k = \alpha$ and $k = \beta$ indicate the positive domain and negative domain, respectively. We will additionally assume that domain α contains bound positive charges, and β contains bound negative charges. The resulting bound charge densities χ^α and χ^β are thus given in terms of their absolute value.

$$j_i^k(\vec{r}) = -D_i\left(\nabla c_i^k(\vec{r}) + \frac{z_i\mathcal{F}c_i^\alpha(\vec{r})}{RT}\nabla\phi^k(\vec{r})\right) \tag{S14}$$

By definition, $\nabla\phi^\alpha(\vec{r}) = \nabla\phi^\beta(\vec{r}) = \nabla\phi(\vec{r})$. Therefore, we can use Equation S4 with Equation S14 to solve for $\nabla\phi(\vec{r})$. Similar to the approach utilized for the uncharged and single-charge membranes, this method will allow j_1 and j_2 to be expressed as functions of the concentrations and concentration gradients.

$$\begin{aligned}
I &= \sum_k^{\alpha,\beta}\sum_i^{1,2} z_i\mathcal{F}j_i^k(\vec{r}) \\
&= z\left(j_1^\alpha(\vec{r}) + j_1^\beta(\vec{r})\right) - z\left(j_2^\alpha(\vec{r}) + j_2^\beta(\vec{r})\right) \\
&= -zD_1\left(\nabla c_1^\alpha(\vec{r}) + \frac{z\mathcal{F}c_1^\alpha(\vec{r})}{RT}\nabla\phi(\vec{r})\right) + zD_2\left(\nabla c_2^\alpha(\vec{r}) - \frac{z\mathcal{F}c_2^\alpha(\vec{r})}{RT}\nabla\phi(\vec{r})\right) \\
&\quad -zD_1\left(\nabla c_1^\beta(\vec{r}) + \frac{z\mathcal{F}c_1^\beta(\vec{r})}{RT}\nabla\phi(\vec{r})\right) + zD_2\left(\nabla c_2^\beta(\vec{r}) - \frac{z\mathcal{F}c_2^\beta(\vec{r})}{RT}\nabla\phi(\vec{r})\right) \\
&= 0
\end{aligned} \tag{S15}$$

Therefore,

$$\begin{aligned}
D_1\left(\nabla c_1^\alpha(\vec{r}) + \nabla c_1^\beta(\vec{r})\right) - D_2\left(\nabla c_2^\alpha(\vec{r}) + \nabla c_2^\beta(\vec{r})\right) \\
= -\frac{z\mathcal{F}}{RT}\left(D_1 c_1^\alpha(\vec{r}) + D_2 c_2^\alpha(\vec{r}) + D_1 c_1^\beta(\vec{r}) + D_2 c_2^\beta(\vec{r})\right)\nabla\phi(\vec{r})
\end{aligned} \tag{S16}$$

The assumption of electroneutrality within the membrane volume implies that the charges in each domain must be balanced, such that

$$0 = zc_1^\alpha(\vec{r}) - zc_2^\alpha(\vec{r}) + \chi^\alpha(\vec{r}) \tag{S17}$$

$$0 = zc_1^\beta(\vec{r}) - zc_2^\beta(\vec{r}) - \chi^\beta(\vec{r}) \tag{S18}$$

which for membranes with charges distributed evenly over their thickness implies

$$\nabla c_1^\alpha(\vec{r}) = \nabla c_2^\alpha(\vec{r}) \qquad \text{and} \qquad \nabla c_1^\beta(\vec{r}) = \nabla c_2^\beta(\vec{r}) \tag{S19}$$

These relationships are used to simplify the left hand side of Equation S16, resulting in

$$\frac{z\mathcal{F}}{RT}\nabla\phi(\vec{r}) = \frac{-(D_1 - D_2)\left(\nabla c_1^\alpha(\vec{r}) + \nabla c_1^\beta(\vec{r})\right)}{\sum_k^{\alpha,\beta}\sum_i^{1,2} D_i c_i^k(\vec{r})} \tag{S20}$$

Substituting Equation S20 into Equation S14, yields

$$j_1^\alpha(\vec{r}) = -D_1\left[\nabla c_1^\alpha(\vec{r}) - c_1^\alpha(\vec{r})\frac{(D_1 - D_2)\left(\nabla c_1^\alpha(\vec{r}) + \nabla c_1^\beta(\vec{r})\right)}{\sum_k^{\alpha,\beta}\sum_i^{1,2} D_i c_i^k(\vec{r})}\right] \tag{S21}$$

$$j_1^\beta(\vec{r}) = -D_1\left[\nabla c_1^\beta(\vec{r}) - c_1^\beta(\vec{r})\frac{(D_1 - D_2)\left(\nabla c_1^\alpha(\vec{r}) + \nabla c_1^\beta(\vec{r})\right)}{\sum_k^{\alpha,\beta}\sum_i^{1,2} D_i c_i^k(\vec{r})}\right] \tag{S22}$$

Rearranging in terms of c_1^α and c_1^β using Equations S17-S18 yields

$$j_1^\alpha(\vec{r}) = -D_1 \left[\frac{\left(2D_2 c_1^\alpha(\vec{r}) + (D_1+D_2)\, c_1^\beta(\vec{r}) + \frac{D_2}{z}\left(\chi^\alpha(\vec{r}) - \chi^\beta(\vec{r})\right)\right)\nabla c_1^\alpha(\vec{r}) - (D_1-D_2)\, c_1^\alpha(\vec{r})\,\nabla c_1^\beta(\vec{r})}{(D_1+D_2)\left(c_1^\alpha(\vec{r}) + c_1^\beta(\vec{r})\right) + \frac{D_2}{z}\left(\chi^\alpha(\vec{r}) - \chi^\beta(\vec{r})\right)} \right] \tag{S23}$$

$$j_1^\beta(\vec{r}) = -D_1 \left[\frac{\left(2D_2 c_1^\beta(\vec{r}) + (D_1+D_2)\, c_1^\alpha(\vec{r}) + \frac{D_2}{z}\left(\chi^\alpha(\vec{r}) - \chi^\beta(\vec{r})\right)\right)\nabla c_1^\beta(\vec{r}) - (D_1-D_2)\, c_1^\beta(\vec{r})\,\nabla c_1^\alpha(\vec{r})}{(D_1+D_2)\left(c_1^\alpha(\vec{r}) + c_1^\beta(\vec{r})\right) + \frac{D_2}{z}\left(\chi^\alpha(\vec{r}) - \chi^\beta(\vec{r})\right)} \right] . \tag{S24}$$

Summing these equations into the total flux results in

$$\begin{aligned} j_1(\vec{r}) &= j_1^\alpha(\vec{r}) + j_1^\beta(\vec{r}) \\ &= -D_1 D_2 \left[\frac{2\left(c_1^\alpha(\vec{r}) + c_1^\beta(\vec{r})\right) + \frac{1}{z}\left(\chi^\alpha(\vec{r}) - \chi^\beta(\vec{r})\right)}{(D_1+D_2)\left(c_1^\alpha(\vec{r}) + c_1^\beta(\vec{r})\right) + \frac{D_2}{z}\left(\chi^\alpha(\vec{r}) - \chi^\beta(\vec{r})\right)} \right] \nabla\left(c_1^\alpha(\vec{r}) + c_1^\beta(\vec{r})\right) \end{aligned} \tag{S25}$$

For a charge-patterned membrane with equal coverage of oppositely-charged domains that do not interact within the membrane, $\int_V \chi(\vec{r})\, d\vec{r} = \left(\chi^\alpha(\vec{r}) - \chi^\beta(\vec{r})\right) = 0$. If we choose the y-direction normal to the membrane, and assume no other spatial variation in the concentration of the membrane (tantamount to "coarse-graining" the membrane's structure into a homogeneous continuum), the gradient term ∇c_1 becomes dc_1/dy

$$j_1(x) = -D_1 D_2 \left(\frac{2}{D_1+D_2}\right) \frac{dc_1(x)}{dy} . \tag{S26}$$

Note that this is the same result as the uncharged membrane, except that the concentration, and therefore overall flux in the membrane is a function of the x position. As expressed in the main text, it is the ion partitioning that dominates the transport of ions through these membranes, which this equation strongly reiterates.

Equations S11, S9, and S26 can be integrated along the thickness of the membrane to express the flux of ions through the uncharged, single-charge, and charge-patterned membranes, respectively, as a function of bulk concentration using the partitioning equations described in the main text.

---

[1] E. L. Cussler and E. L. Cussler, *Diffusion: Mass Transfer in Fluid Systems*, Cambridge Series in Chemical Engineering (Cambridge University Press, 1997).

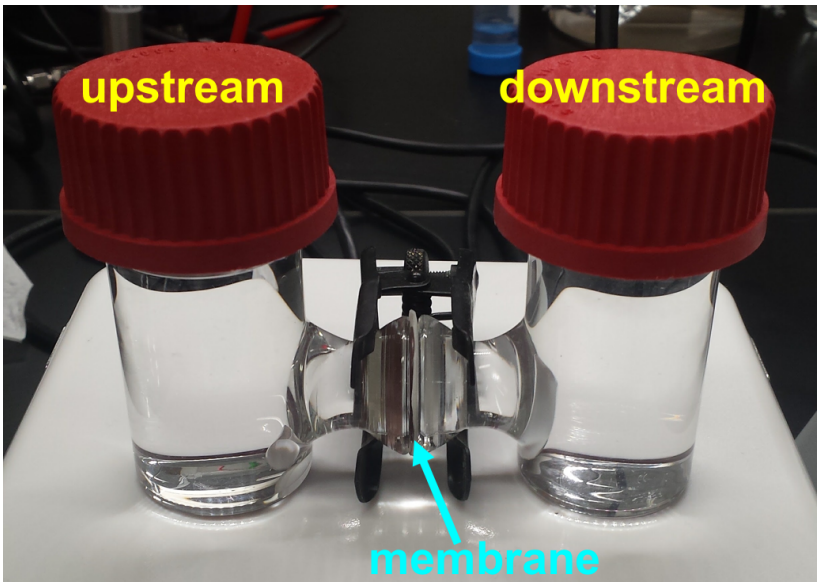

FIG. S1. Photograph of the home-built diffusion cell system used to quantify the salt permeability values of membranes. A membrane is placed between the two reservoirs. The exposed membrane area was equal to 0.97 cm^2. The left reservoir, referred to as the upstream, contains an aqueous solution at a known salt concentration, while the right reservoir, denoted as the downstream, contains only DI water to start. The upstream and downstream reservoirs each contained 20 mL of the respective solutions. The concentration in the downstream is monitored over time using a conductivity probe and/or removing samples for ICP-OES analysis. 200 µL samples were withdrawn for ICP-OES analysis and replaced with an equivalent volume of DI water to maintain a constant solution volume.

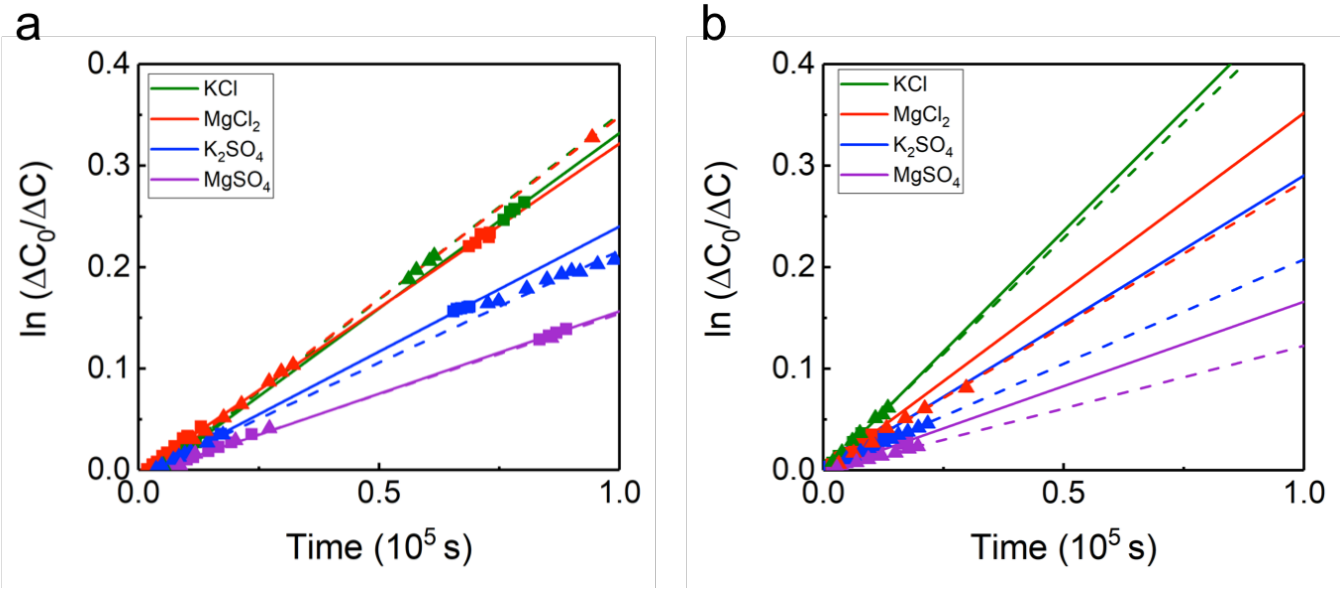

FIG. S2. Representative results from diffusion cell experiments. In the cases shown here, the diffusion cell experiments were executed with uncharged membranes and an upstream solution containing a single salt. The upstream reservoir was filled with a salt solution at an initial concentration of 10 mM (a) or 100 mM (b). Four salts were studied in separate trials. Uncharged membranes were prepared by printing a poly(ethylene oxide)/poly(vinyl alcohol) (PEO/PVA) composite ink on a polycarbonate track-etched membrane to produce similar pore sizes to those of charged membranes without imprinting a surface charge. The solid lines correspond to the results from a single membrane; the dashed lines correspond to a second membrane tested under the same conditions. The 100 mM experiments were terminated after reaching sufficiently high downstream salt concentrations, which occured within a few hours. However, the trendlines are extended in order to more easily compare the results from the 100 mM experiments with the results from the 10 mM experiments.

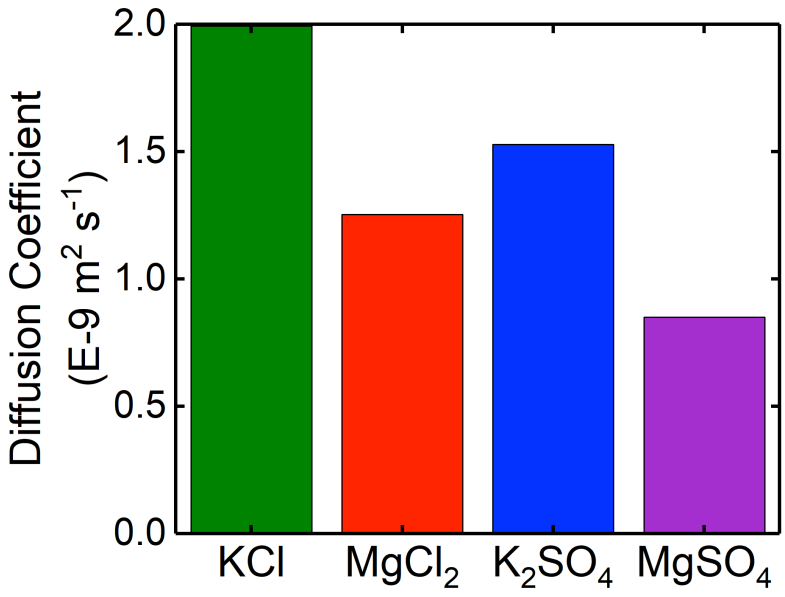

FIG. S3. The values of the diffusion coefficients in water for the four salts used in this study.[1]

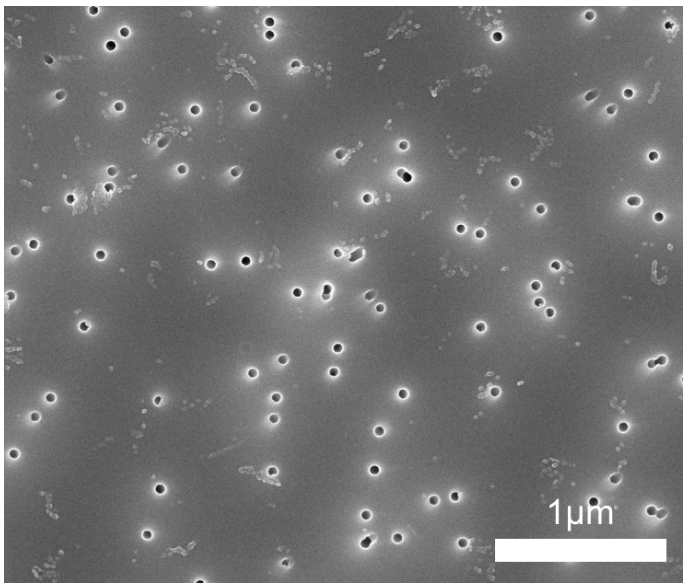

FIG. S4. A scanning electron micrograph (SEM) of a bare 50 nm polycarbonate track-etched substrate. Membranes were fabricated by printing composite ink(s) onto this track-etched template. ImageJ software was used to analyze the porosity of the substrate. The value of the porosity was found to be approximately 2%, which is in good agreement with 0.6% reported by manufacturer.

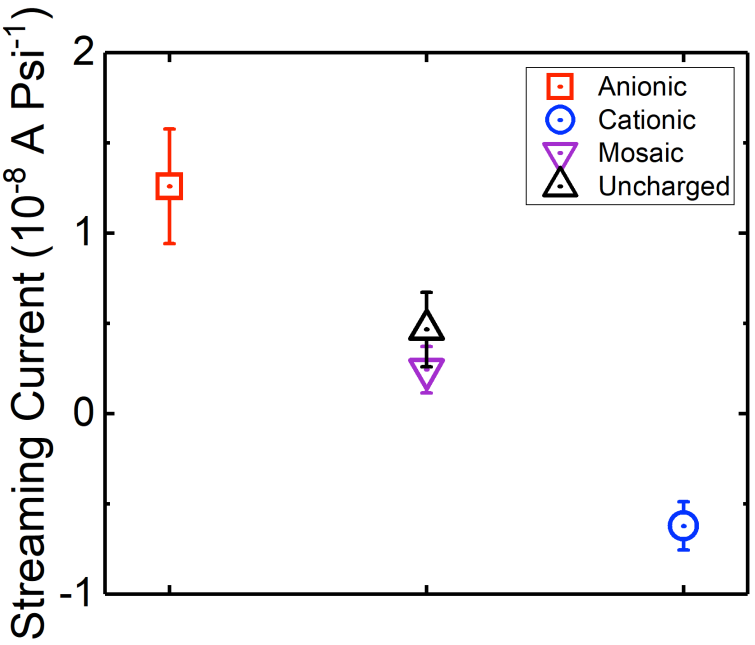

FIG. S5. Average streaming current values normalized by applied pressure for the different membrane types. Due to the experimental set-up, a negative streaming current indicates a positive surface charge and *vice versa*. Error bars represent one standard deviation based on at least three membranes. There exists a slight imbalance in magnitude of streaming current for the anionic and cationic membranes, likely due to the native negative surface charge of the polycarbonate substrate. However, both the mosaic and the uncharged membranes have a nearly zero streaming current, implying a net neutral surface.

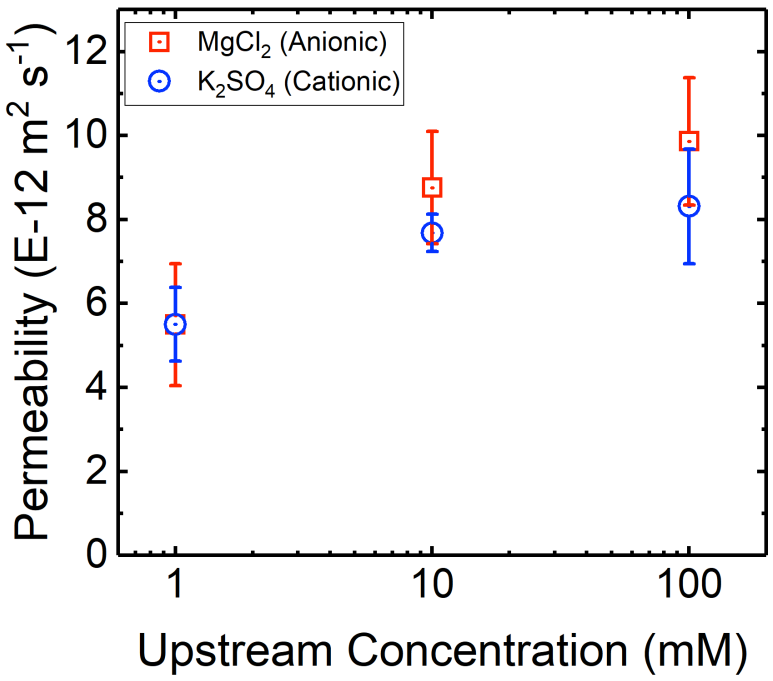

FIG. S6. Permeability of $MgCl_2$ through anionic membranes and K_2SO_4 through cationic membranes at varying concentrations. These values were measured using diffusion cell experiments. The asymmetric salt with the divalent counter-ion had the highest permeability through single-charge membranes. Error bars represent one standard deviation from the mean based on at least three membranes.

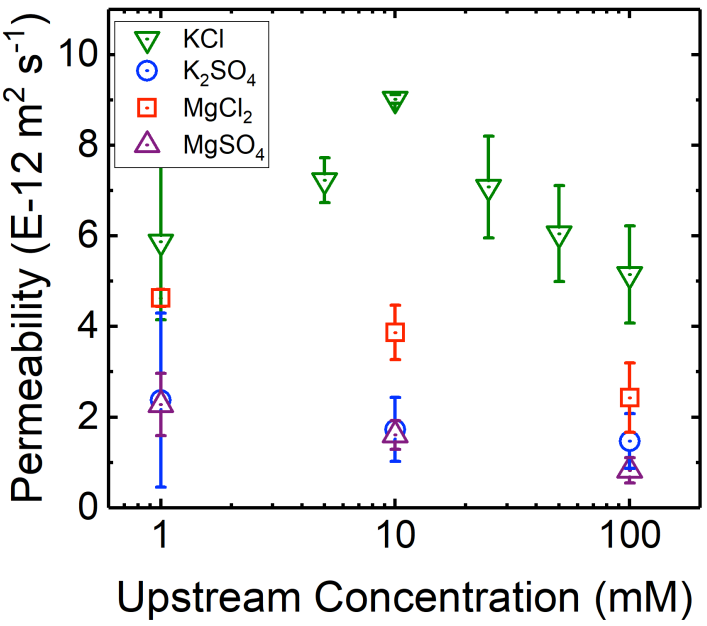

FIG. S7. Salt permeability of four salts through charge-patterned mosaic membranes as a function of salt concentration. The permeability was calculated from diffusion cell experiments with varying upstream salt concentrations. DI water was used as the downstream solution. Error bars represent one standard deviation from the mean based on at least three membranes.

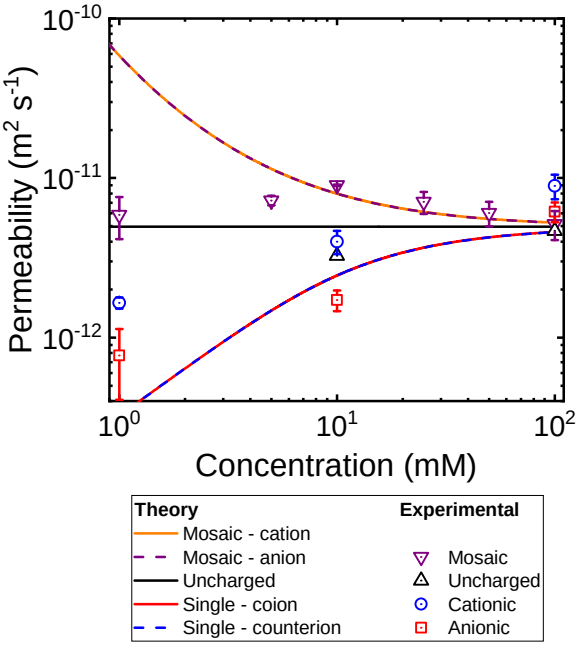

FIG. S8. Experimental permeability values for KCl from diffusion cell experiments (shown in Fig. 4) superimposed on the results of the mathematical model displayed in Fig. 2b. The model is scaled by the porosity of a modified membrane (0.25%).

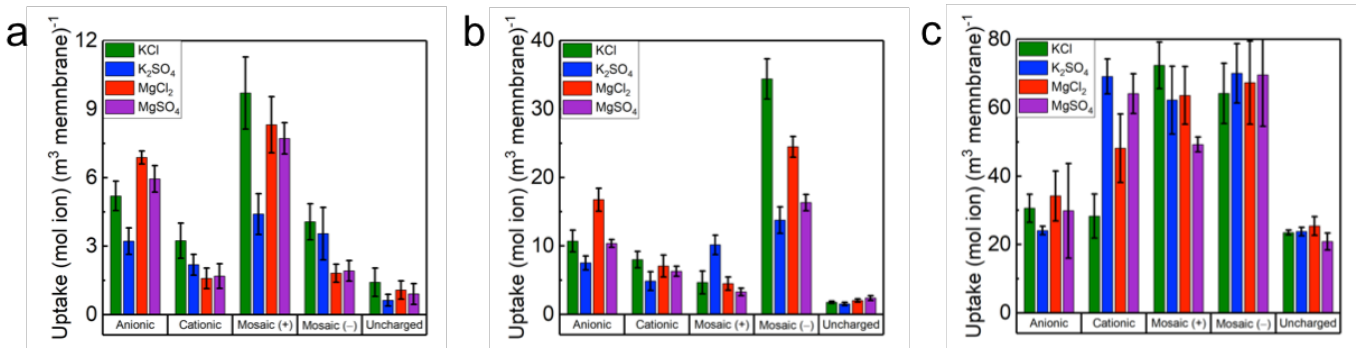

FIG. S9. 1 mM (a), 10 mM (b), and 100 mM (c) sorption experiments for four salts for four different membranes. Uptake is in moles of counter-ion for anionic and cationic membranes. Uptake of cations and anions by the charge-patterned mosaic membranes were measured independently and reported as mosaic (+) and mosaic (−), respectively, and normalized by the fraction of surface coverage. The concentration of cations were measured for the uncharged membranes. Error bars represent one standard deviation from the mean taken from at least three membranes.

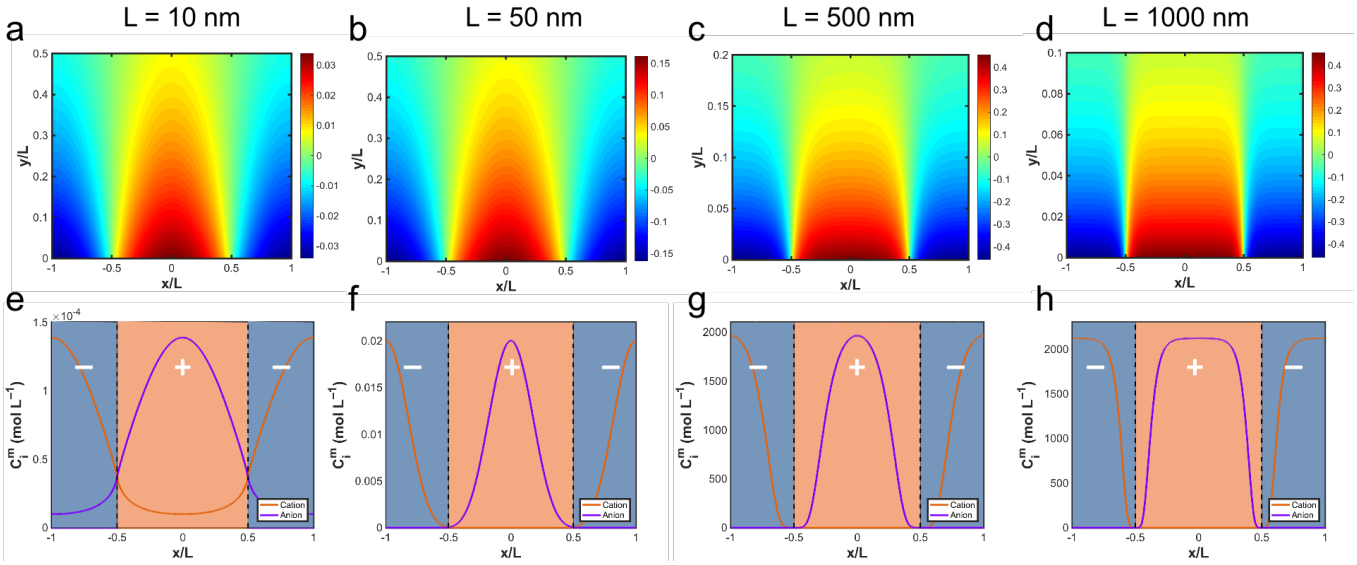

FIG. S10. Electrostatic potential (mV) for charge-patterned mosaic membranes for stripe widths of (a) $L = 10\,\text{nm}$, (b) $L = 50\,\text{nm}$, (c) $L = 500\,\text{nm}$, and (d) $L = 1\,\mu\text{m}$ for a constant 50 nm Debye length. The x and y values are normalized by the stripe width, L. (e)–(h) Plots of normalized concentration as a function of position along the surface of the membrane ($y = 0$) corresponding to the respective values of L and λ_D in (a)–(d). c_i^m and c_b are the concentrations of ions in the membrane and bulk solutions, respectively. The blue and orange shaded regions correspond to the negative and positive domains, respectively, as shown in Fig. 1.

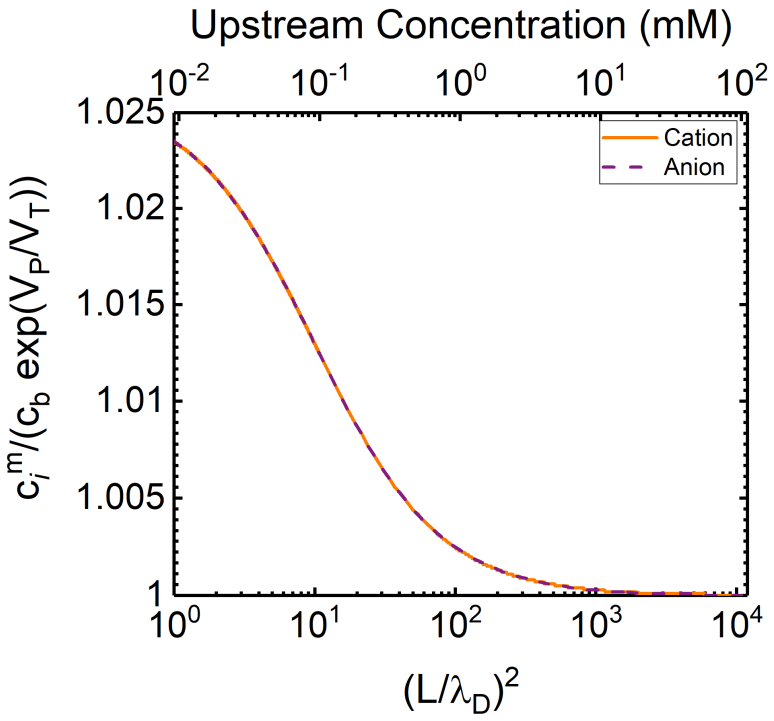

FIG. S11. Dimensionless partitioning of cations and anions in a charge-patterned mosaic membrane as a function of the two characteristic lengths: stripe width, L, and Debye length, λ_D. The associated upstream concentrations (assuming $L = 100nm$) are plotted as a second x-axis. $V_P = \frac{4\sigma_0 L}{\pi\epsilon}$ and $V_T = \frac{z\mathcal{F}}{RT}$ are the pattern and thermal voltages, respectively, while c_i^m and c_b are the concentrations in the membrane and the bulk of the upstream solution, respectively.

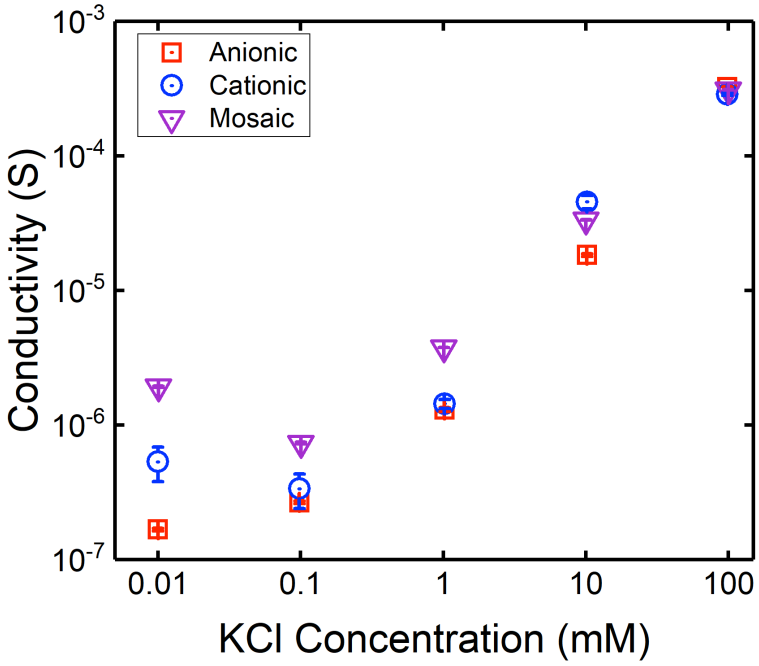

FIG. S12. Conductivity as a function of KCl concentration for three types of membranes. Conductivity is measured by taking the slope of an IV curve at the given KCl concentration. Average and standard deviations were taken from measuring the IV curves at each concentration at least three times.